Cellulose (2017) 24:4449–4459
DOI 10.1007/s10570-017-1423-6

ORIGINAL PAPER

Preparation and properties of microcrystalline cellulose/hydroxypropyl starch composite films

Jie Chen · Zhu Long · Jianhua Wang · Meiyan Wu · Feng Wang · Bin Wang · Wenzhi Lv

Received: 25 April 2017 / Accepted: 20 July 2017 / Published online: 31 July 2017

Abstract In this paper, microcrystalline cellulose (MCC)/hydroxypropyl starch (HPS) composite films are prepared by the solution casting method, and the effect of different amounts of microcrystalline cellulose on the properties of the films is investigated. The structure of MCC/HPS composite materials is characterized by Fourier transform infra-red and scanning election microscopy, and thermal stability, mechanical properties, hygroscopicity, and water vapor permeability of the composite films are also tested. According to the test results, with increasing MCC amounts, glass transition temperature, thermal stability, and tensile strength of MCC/HPS composite films are improved, while the hygroscopicity and water vapor permeability of MCC/HPS composite materials are decreased. When the content of MCC reaches 6 wt%, the maximum increase of the glass transition temperature is about 9.63 °C, and the tensile strength of MCC/HPS composite films are increased by 300% compared with that of HPS films. Moreover, the addition of MCC helps to expand the application of hydroxypropyl starch in the packaging field.

Keywords Microcrystalline cellulose · Hydroxypropyl starch · Composite film · Tensile strength · Thermal stability

J. Chen · Z. Long (✉) · M. Wu · F. Wang · W. Lv
Key Laboratory of Eco-textiles, Ministry of Education, Jiangnan University, Wuxi 214122, China
e-mail: longzhu@jiangnan.edu.cn

J. Chen · Z. Long · B. Wang · W. Lv
State Key Laboratory of Pulp and Paper Engineering, South China University of Technology, Guangzhou 510640, China

J. Wang
Zhejiang Yongtai Paper Group Stock Co., Ltd., Fuyang 311421, Zhejiang Province, China

Introduction

As society develops and quality of life improves, people's environmental awareness gradually increases. To combat the use of non-biodegradable materials prepared by chemical polymer synthesis (Yoon et al. 2012), people now are devoted to seeking environment-friendly packaging, which is safe, pollution-free, and biodegradable (Bergo et al. 2008).

In fact, starch, a low-cost, biodegradable, and renewable natural resource that is widely distributed in nature and produces little waste, is universally recognized as a promising representative of novel biodegradable materials (Brandelero et al. 2016). Because the numerous hydroxyl groups in starch form hydrogen bonds between molecules, starch does not have thermoplastic properties. In additon, starch is also characterized by high brittleness, poor mechanical properties, and low water resistance due to aging and hydrophilicity (Bakrudeen et al. 2016). In recent years, many scholars have adopted mineral or

cellulose fillers to change the properties of starch films (Brandelero et al. 2015; Lim et al. 2016; Rahman et al. 2010). For example, Cervantes-Sanchez used MFC (microfibrillated cellulose) as a filler and added it to a wheat starch solution plasticized by polyols (glycerol and sorbitol) with different molecular weights, thus improving rigidity and water absorption resistance of composite materials with increasing MFC amounts (Cervantes-Sanchez et al. 2016). Adriana Nicoleta Frone investigated the effect of different amounts of cellulose nanofibers (CNF) on thermal stability of starch/polyvinyl alcohol (S/PVA) via the one-pot method (Frone et al. 2015). Lani studied the effect of nanocellulose isolated from empty fruit bunch (EFB) fiber on polyvinyl alcohol (PVA)/starch blend films (Lani et al. 2014). Dufresne and Vignon added MFC to potato starch, improving thermal mechanical properties, reducing water sensitivity, and maintaining biodegradability of films (Dufresne and Vignon 1998). Yano and Nakahara added 2 wt% wheat straw nanocellulose to oxidized cassava starch, whereby doubled yield strain of composite materials and increased bending degree significantly (Yano and Nakahara 2004). Mondrago'n put 2 wt% MFC suspensions into molten thermoplastic starch, thereby enhancing the tensile strength, as well as rigidity of composite materials (Lavoine et al. 2012). Svagan put 70 wt % MFC into amylopectin-glycerol, increasing tensile strength and reducing the water diffusion rate of composite materials (Svagan et al. 2009).

Hydroxypropyl starch, a type of water-soluble starch derivative, was used as matrix. With hydrophilic hydroxypropyl groups introduced into hydroxypropyl starch molecules under alkaline conditions, hydroxypropyl starch belonged to nonionic starch ether with good anti-acid, anti-alkali, and anti-salt, and good resistance to polyvalent metal ions. Furthermore, the high stability of substituted ether bonds in turn increased the freeze–thaw stability of starch and improves properties of formed films. At present, the composite materials on the market were mainly starch-based composite films, but very few hydroxypropyl starches were used as substrates for the preparation of composites. Currently, hydroxypropyl starch, as a binder, thickener, and suspending agent, and other food additives are widely used in the food industry. Considering the stability of hydroxypropyl starch paste, film formation of the paste was good, and the prepared films were transparent, flexible, smooth, had good folding resistance, and were water-soluble, so they were chosen to for application in edible food packaging materials in this study. Nevertheless, the shearing resistance and thermal stability of modified starch were poor (Fouladi and Nafchi 2014; Lawal 2011; Lee and Yoo 2011). Accordingly, micro-particles were added so as to strengthen the mechanical properties and thermal stability of hydroxypropyl starch films.

Microcrystalline cellulose, the product of natural cellulose hydrolyzed by acid (Brannan et al. 2014; Siqueira et al. 2010), was characterized by low cost, low density, high specific surface area, high strength, high elastic modulus, high thermal stability, biodegradability, and recyclability (Andresen et al. 2006; Czaja et al. 2007; Dufresne et al. 2000; Siro and Plackett 2010). In order to improve the performance of hydroxypropyl starch-based film, organic filler microcrystalline cellulose was added, which increased the mechanical properties and decreased the water vapor permeability and migration resistance to broaden further the scope of hydroxypropyl starch in the field of green food packaging.

Therefore, the advantages of hydroxypropyl starch and microcrystalline cellulose were combined in this paper. With hydroxypropyl starch as the base material, microcrystalline cellulose as the filler, glycerol and water as plasticizer, composite films of microcrystalline cellulose/hydroxypropyl starch were prepared by the simple method of casting, which is a commonly used method for laboratory film formation.

Experimental

Materials

Microcrystalline cellulose was purchased from Tianjin Guangfu Fine Chemical Research Institute. The molecular weight was 31,439.64, the degree of polymerization was approximately 194, the pH value of 10% aqueous suspension was 7, and the granularity was 20–100 μm. Hydroxypropyl starch was purchased from Zhengzhou Shiquanshimei Trading Co., Ltd, and the molecular weight was 18,657. Analytically pure glycerol was purchased from Sinopharm Chemical Reagent Co., Ltd, and the molecular weight was 92.09. We used deionized water in the experiment.

Preparation of MCC/HPS composite films

First, 5 wt% HPS solution was prepared, and 20 wt% glycerol was added (accounted for in the weight of HPS), then they were mixed evenly by a glass rod. Then the solution was placed in a water bath of 70 °C and stirred for 10 min. Later, the temperature of the water bath was transferred to 95 °C, and the solution was stirred continuously for 30 min to gelatinize. Meanwhile, 20 mL of deionized water was added to different amounts of microcrystalline cellulose respectively (0, 3, 6, and 9 wt%, accounted for in the weight of HPS) and ultrasonicated for 30 min at 380 W. After that, the microcrystalline cellulose suspension was added to the gelatinized HPS solution followed by 30 min of magnetic stirring at a temperature of 95 °C. After 45 min of slow stirring at 45 °C, the mixed solution 100 mL of the gelatinized solution was poured into a Teflon mold then dried in an air oven at 60 °C, finally producing that films.

Morphological analysis

The surfaces of thin composite films were spray-coated with gold. Then scanning election microscopy (Hitachi SU 1510, Japan) was employed to observe the microscopic morphology with an accelerating voltage of 5 kV.

Fourier transform infra-red (FT-IR) analysis

Fourier Transform Infra-red Spectrometer (Nicolet Nexus, Thermo Electron Corporation, Waltham, MA, USA) was used to test samples with the wavelength ranging from 400 to 4000 cm^{-1} and a resolution of 4 cm^{-1}.

Differential scanning calorimeter (DSC) analysis

Differential scanning calorimetry (Q200, American TA Instrument Corporation, USA) was use to test samples under a N_2 atmosphere, with the temperature ranging from 30 to 260 °C and a heating rate at 10 °C/min.

Thermogravimetric analysis (TGA)

Thermogravimetry (TGA/TA-Q500, Newcastle, UK) was employed to test samples under a N_2 atmosphere, with the temperature ranging from 30 to 600 °C and a heating rate at 10 °C/min.

Mechanical properties

First, the prepared composite films were cut into strips in the size of 100 mm × 15 mm (length × width). Second, the thickness of each strip was tested using a coated thickness meter (MP 0, Fiscfer Company, Germany), the value of which ranged from 0.17 to 0.21 mm. Finally, a tensile test of the strips was conducted using a universal testing machine (KDII-0.05, China), with a clamping length of 50 mm and a tensile speed of 10 mm/min. During the test, three parallel tests were performed to ensure the feasibility of the measurement results.

Moisture content

The mass of sample films before and after drying for 5 h at 105 °C in an oven was measured to determine the moisture content, which was calculated by the following formula:

$$\text{Moisture content} = \frac{m_1 - m_0}{m_0} \times 100\% \quad (1)$$

In formula (1), m_0 represents the mass of sample films before drying; m_1 represents the mass after drying.

Moisture absorption

Firstly, the composite films were cut into 30 mm × 30 mm samples and placed in a 40 °C oven, then weighed after being completely dried, the mass of which marked as M_d. Secondly, the samples were placed in desiccators of inorganic salt saturated solutions (59 and 75% of relative humidity, separately) containing sodium bromide and sodium chloride, respectively. Then, the samples were taken out at intervals and weighed immediately, the mass of which marked as M_W. The hygroscopicity percentage of unit mass, namely the hygroscopicity rate, was marked as M_C (Alhuthali et al. 2012).

$$M_c = \frac{M_w - M_d}{M_d} \times 100\% \quad (2)$$

Water vapor permeability

First, the tested films were placed in an environment (25 °C) with relative humidity at 59% for

48 h to balance the moisture content. Second, 10 g of dried calcium chloride was used as desiccant and placed in a weighing bottle. Third, the weighing bottles were sealed by the prepared films to be tested, ensuring an effective area of 19.625 cm^2 for each sample film. Fourth, the weight of each sealed bottle was measured accurately to 0.0001 g. Finally, the bottles were placed in a desiccator containing saturated sodium chloride solution (75% RH) and saturated potassium nitrate solution (95% RH), and the mass of bottles was measured every 24 h until stable.

The formula for calculating the water vapor transmission (WVT) of samples is as follows (Guz et al. 2017):

$$\mathrm{WVT} = \frac{24 \cdot \Delta m}{A \cdot t} \tag{3}$$

In formula (3), *WVT* represents the water vapor transmission ($g/m^2/s$); t represents the time interval between two mass increments (s); Δm represents the mass increment during the period of t (g); and A refers to the area of samples permeated by water vapor (m^2).

The formula for calculating the water vapor permeability (WVP) of samples is as follows:

$$\mathrm{WVP} = \frac{\mathrm{WVT} \cdot d}{24 \cdot P \cdot (R_1 - R_2)} \tag{4}$$

In formula (4), *WVP* represents the water vapor permeability ($g/m^2/s/Pa$); d represents the sample depth (m); P refers to the saturation pressure of water vapor at a temperature of 25 °C (Pa); R_1 refers to the relative humidity of the test environment (%); and R_2 refers to the relative humidity of the inner environment of weighing bottles (%).

Solvent resistance and absorption

Acetone, petroleum ether, ethyl alcohol, oleic acid, and xylene were used to test the solvent resistance and absorption of all the films. Film samples were immersed in different solvents at 30 °C for 48 h, and they were observed with a camera to reflect the solvent resistance properties. The solvent absorption of the films was showed by the initial film weight and the film weight after immersion in solvent for a certain. The solvent absorption ratio (SAR, %) was calculated using the following equation:

$$\mathrm{SAR} = \frac{w_t - w_0}{w_0} \times 100\% \tag{5}$$

where w_0 is the initial weight of the films; w_t is the weight of the films took out from the solvent.

Results and discussion

Morphological analysis of composite films

The surface SEM diagrams of microcrystalline cellulose composite films in different proportions are shown in Fig. 1. Figure 1a shows the HPS films. The surface of prepared films was relatively smooth due to the high solubility of hydroxypropyl starch and cross-linking reaction among starch molecules under the action of plasticizers (water and glycerol). Microcrystalline cellulose particles were found on the surface of the composite films, as shown in Fig. 1b–d. Microcrystalline cellulose was uniformly distributed on the surface of the MCC/HPS composite films due to a small added amount, as demonstrated in Fig. 1b. When the amount of microcrystalline cellulose increased to 6 wt% (Fig. 1c), it was mostly evenly dispersed on the surface of the composite films, and only a few microcrystalline cellulose molecules produced one or two large particles after collision. However, when the content of microcrystalline cellulose reached 9 wt%, microcrystalline cellulose self-aggregation occurred due to uneven distribution. Meanwhile, clusters of large particles were spotted in the composite films resulting in a decrease of surface smoothness (Liu et al. 2013; Ramesan and Surya 2016).

Fourier transform infra-red (FT-IR) analysis of composite films

Infra-red spectra of hydroxypropyl starch films and MCC/HPS composite films are shown in Fig. 2. An obvious O–H stretching vibration absorption peak appeared at 3290 cm^{-1}, showing a hydrogen bond formed between starch and microcrystalline cellulose (Ismail and Zaaba 2014). Nonetheless, the same peak appeared at a lower wavenumber owing to the enlarged combination surface of starch and microcrystalline cellulose with increasing amounts of MCC. More hydrogen bonds thus were formed, which enhanced the binding force between molecules. With

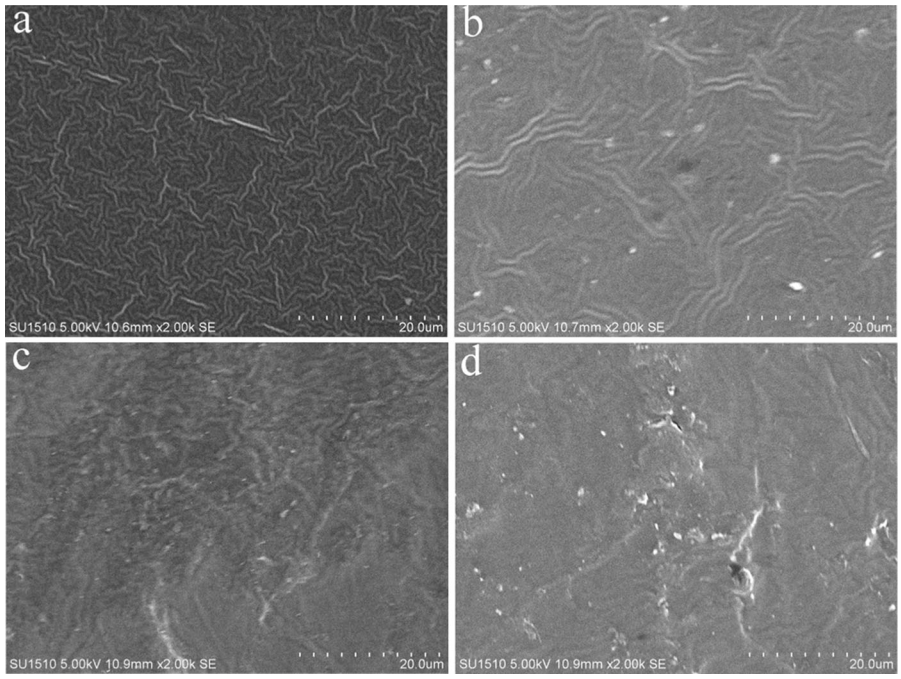

Fig. 1 SEM images of the composite films: **a** HPS films, **b** 3 wt% MCC/HPS composite films, **c** 6 wt% MCC/HPS composite films, **d** 9 wt% MCC/HPS composite films

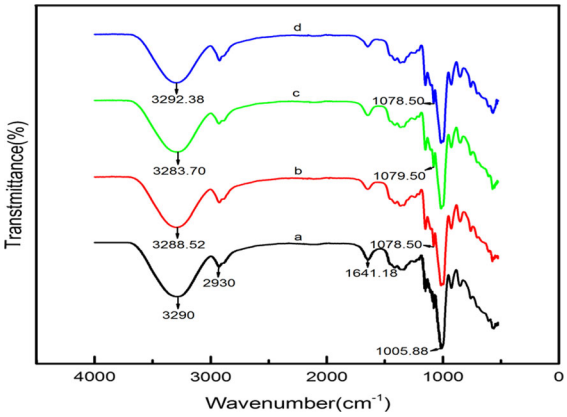

Fig. 2 FTIR spectra of composite films: *a* HPS films, *b* 3 wt% MCC/HPS composite films, *c* 6 wt% MCC/HPS composite films, *d* 9 wt% MCC/HPS composite films

the addition of 9 wt% MCC to the HPS solution, aggregation occurred easily due to the failure of even dispersion of MCC in the HPS solution, increasing the binding distance between starch molecules. Therefore, the O–H absorption peak of the composites was found at a high wavenumber (Lu et al. 2008). The C–O stretching vibration peak formed by starch, microcrystalline cellulose, and glycerol appeared in the range of 1050 to 1080 cm^{-1}. Yet, no obvious absorption peak of HPS films showed around 1078 cm^{-1} in Fig. 2, because the absorption peak here was mainly the C–O stretching vibration peak of microcrystalline cellulose molecules, which contributed to a significantly stronger C–O stretching vibration absorption peak of MCC/HPS composite films than that of HPS films (Yakimets et al. 2007). The stretching vibration peak of saturated C–H on alkyl groups appeared at the wavenumber of 2930 cm^{-1}, while the stretching vibration peak of O–H bond in water molecules formed between molecules appeared at the wavenumber of 1640 cm^{-1}.

The typical absorption peak frequency of HPS films and MCC/HPS composite films experienced little change, as shown in Fig. 2. Thus, mainly playing the role of filler in composite materials, microcrystalline cellulose created few derivatives after addition to hydroxypropyl starch solution for the preparation of composite films (Jang et al. 2007; Sobral et al. 2005).

Differential scanning calorimeter (DSC) analysis of composite films

Figure 3 demonstrated the DSC diagram of original starch films and MCC/HPS composite films. The

decalescence peak appeared at 128.03 °C in the HPS film curve, which referred to the glass transition temperature of HPS films. Nevertheless, the glass transition temperatures of 3, 6, and 9 wt% MCC/HPS composite films were at 135.44, 137.66, and 134.98 °C, respectively. Thus, the glass transition temperatures of prepared composite films all increased after the addition of microcrystalline cellulose to the solution of hydroxypropyl starch, the maximum increase range being 9.63 °C. Microcrystalline cellulose added to the pre-gelatinized hydroxypropyl starch solution can increase the glass transition temperature of the composite films, ascribed to the increase in the number of hydrogen bonds formed between microcrystalline cellulose and starch molecules, restricting the movement of polymer segments. However, when the amount of microcrystalline cellulose increased to 9 wt%, there was a decrease of the glass transition temperature of the composite films due to the cluster phenomenon caused by the addition of excessive microcrystalline cellulose to hydroxypropyl starch solution (Mondragon et al. 2015).

Thermogravimetric analysis (TGA) of composite films

Figure 4 described TGA thermal analysis of HPS films and MCC/HPS films in different proportions. The four top-down curves in the chart reflected the mass change of 9 wt% MCC/HPS composite film, 6 wt% MCC/HPS composite film, 3 wt% MCC/HPS composite film, and HPS film, successively, according to different temperatures. Their trends were roughly the same, presenting a three-segment change. Firstly, the weight

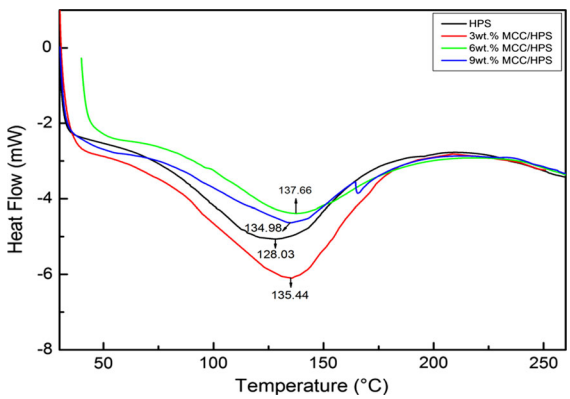

Fig. 3 DSC curves of the composite films

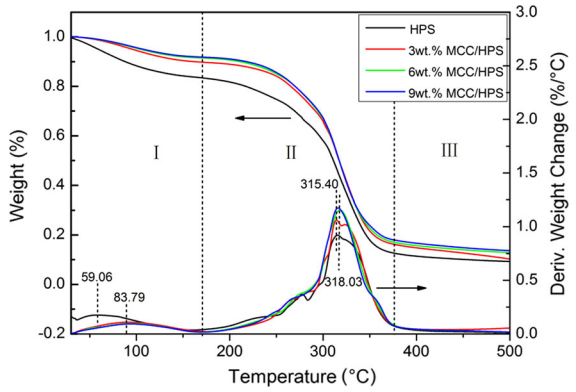

Fig. 4 TGA of the composite films

loss of the first segment appeared in the temperature range of 30–180 °C, the quantity of which ranged from 9 to 18% approximately, and the temperature increased from 59.06 to 83.79 °C. The adsorption of free residual water in the films and the volatilization of glycerol used as plasticizer at high temperature mainly accounted for the loss during the heating process (Ma et al. 2005). Among them, the weight loss of HPS films (17.61%) considerably exceeded that of MCC/HPS (around 9%). These phenomena were facilitated by the gradual enhancement of both intramolecular and intermolecular binding force of MCC, glycerol, and hydroxypropyl starch with increasing amounts of MCC. Next, the weight loss of the second segment appeared in the temperature range of 180–450 °C, being the primary stage for sample mass loss. This mainly refers to the degradation of macromolecular chains formed by hydroxypropyl starch and microcrystalline cellulose in the composite films at high temperature. The improvement of thermal stability of the composite films containing MCC appeared at 318.03 °C due to the addition of MCC, which increased the binding force between molecules of composites, hindered the movement of macromolecular chains, and thereby inhibited the degradation of the films (Frone et al. 2015). Finally, the mass loss appeared in the temperature range of 450–600 °C, during which much carbon residue was generated.

Judging from TGA and DSC diagrams of HPS films and MCC/HPS films in different proportions, the thermal stability of the composite films containing microcrystalline cellulose was significantly higher than that of hydroxypropyl starch films. This was mainly attributed to the addition of microcrystalline cellulose, which increased the number of hydrogen

bonds between molecular chains of starch and microcrystalline cellulose.

Mechanical properties of composite films

Statistics on moisture content, thickness and tensile properties are listed in Table 1.

As can be inferred from Table 1, the decrease of the moisture content of the composite films resulted from the addition of microcrystalline cellulose because of the higher hydrophilicity of hydroxypropyl starch compared to that of microcrystalline cellulose. In addition, the tensile strength of MCC/HPS composite films enhanced with increasing amounts of MCC, and then decreased after reaching a peak (when the MCC amount reached 6 wt%) because the MCC added to hydroxypropyl starch solution facilitated the massive emergence of hydrogen bonds among molecules of starch and microcrystalline cellulose and intensified adhesion between the matric and filler (Rico et al. 2016). With a high crystalline structure, high aspect ratio, and micron effect resulting from its uniform distribution, the characteristics of microcrystalline cellulose might be another cause (Rodionova et al. 2012; Veigel et al. 2011). Aggregation of some MCC occurred when 9 wt% MCC was added to the mixed solution, reducing the effective contact area between microcrystalline cellulose and substrate starch. Failure to function as a binder then led to the reduction of tensile strength of the composite films. On the other hand, elongation at a break of the composite films decreased with increasing amounts of MCC. Consequently, the addition of MCC not only failed to improve the flexibility of the composite films, but also increased its rigidity, the result of which was attributed to the rigidity of MCC itself, the formation of a rigid network structure of MCC and hydroxypropyl starch, and the decrease in moisture content in the prepared composite films (Fukuzumi et al. 2013).

Moisture absorption of composite films

The moisture absorption of different composite films in the environments of 59% RH and 75% RH is described in Fig. 5. The moisture absorption of composite films decreased gradually with the increase in microcrystalline cellulose. After the HPS films were placed in environments of 59% RH and 75% RH for 12 h, their hygroscopicity rate reached the highest (9.79 and 15.25%, respectively); that of 6 wt% MCC/HPS composite films was the lowest (8.08 and 11.64% respectively), decreasing by 17.47 and 31.01% separately. This is because the gradually increasing amounts of MCC promoted the formation of more hydrogen bonds between starch and MCC molecules and improved the compactness of the composite films (Edhirej et al. 2017). By contrast, the hygroscopicity of the composite films with large amounts of MCC was poor, caused by the lower hydrophilicity of MCC compared to that of hydroxypropyl starch. Nonetheless, failing to form a compact network structure, the 9 wt% MCC tended to produce large particles in the matrix, resulting in a higher hygroscopicity of 9 wt% MCC/HPS composite films compared to that of 6 wt%

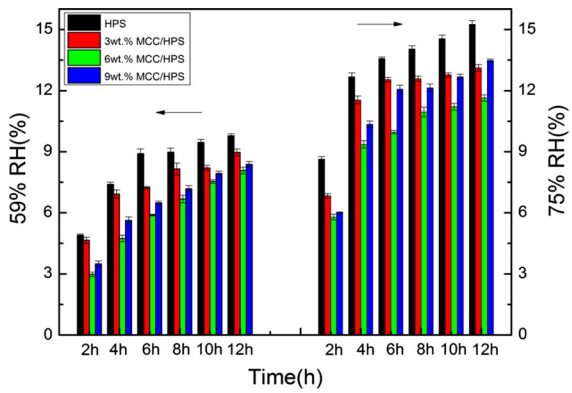

Fig. 5 Moisture absorption properties of composite films in different humidity environments

Table 1 Water content and tensile properties of films prepared form HPS and MCC

Types of samples	Moisture content (%)	Thickness of films (mm)	Tensile strength (MPa)	Elongation at break (%)
HPS	18.67 ± 0.56	0.21 ± 1.2	2.97 ± 0.28	60.08 ± 1.84
3 wt% MCC/HPS	11.87 ± 0.74	0.20 ± 1.6	6.25 ± 0.80	8.15 ± 0.91
6 wt% MCC/HPS	10.69 ± 0.35	0.18 ± 0.7	12.54 ± 1.26	6.98 ± 2.04
9 wt% MCC/HPS	8.74 ± 0.11	0.17 ± 0.9	9.77 ± 0.84	4.87 ± 0.66

MCC/HPS films (Ramaraj 2006). The hygroscopicity of composite films in the high humidity environment was much higher than that in the low humidity environment, as also demonstrated in Fig. 5. Hydroxypropyl starch as a kind of hydrophilic starch derivative and MCC as hydrophilic substance were two main reasons for this (Liu et al. 2014).

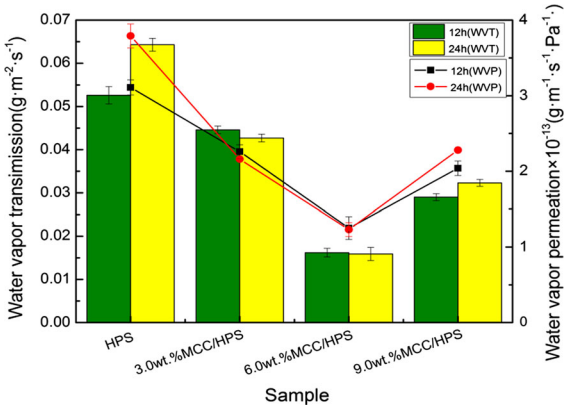

Fig. 6 Water vapor permeation of composite films at different times in 75% RH

Water vapor permeability of composite films

The water vapor permeability of composite films placed in the envi samples were placed in an environment of 59% RH for 48 h in advance for moisture balance before testing. The water vapor permeability of composite films decreased with increasing amounts of MCC in hydroxypropyl starch solution. The addition of MCC, on the one hand, enhanced the binding force between MCC and hydroxypropyl starch molecules, forming a dense composite film. On the other hand, the water vapor transmission path in the composite films was prolonged, and the amount of water vapor permeating through the films decreased in a certain period of time due to the uniform distribution of MCC in the starch matrix as a filler (Kaushik and Kaur 2016). However, the water vapor permeability of samples containing

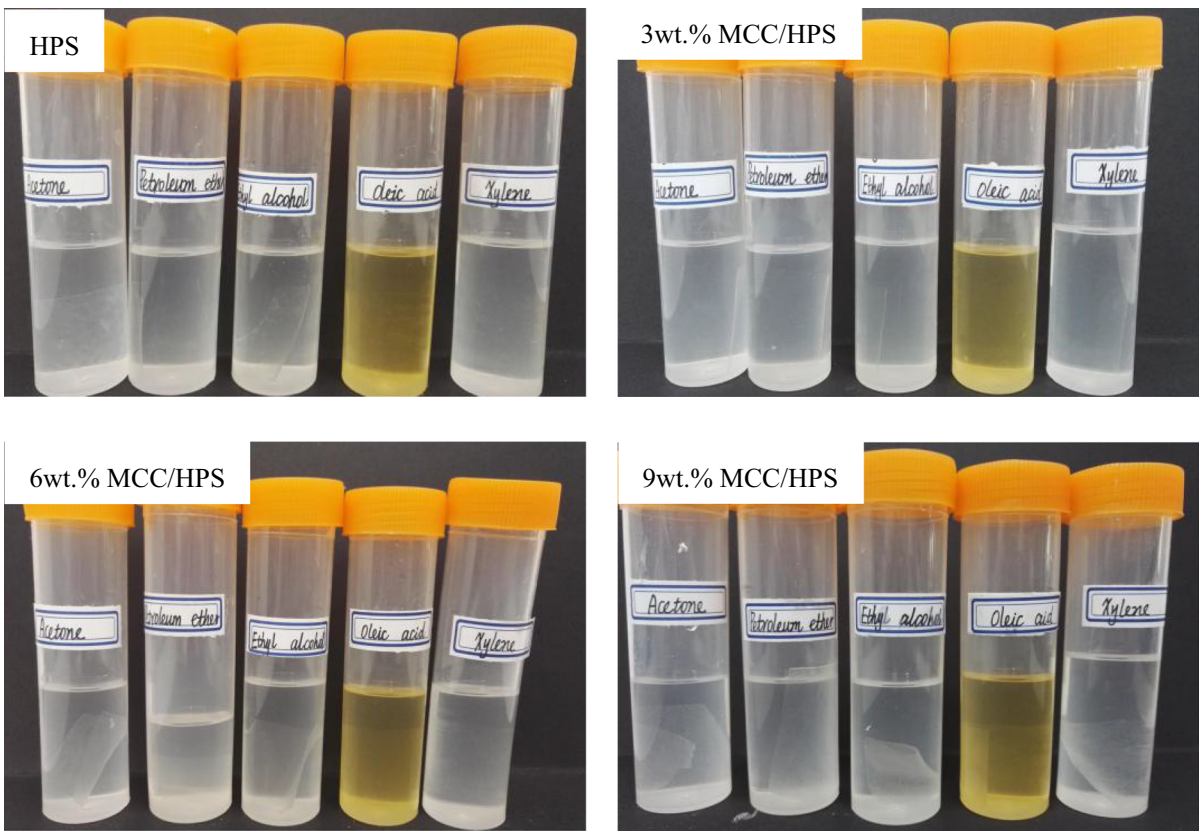

Fig. 7 Solvent resistance of MCC/HPS films after 48 h

9 wt% MCC was higher than that of samples containing 6 wt% MCC, as shown in Fig. 6. The cause lay in the cluster phenomenon appearing after the addition of 9 wt% MCC to the matrix, producing larger pores which allowed a massive quantity of water vapor to permeate through composite films via a shorter path and increased the water vapor transmission within a certain period of time (Brandelero et al. 2010). The water vapor permeability of some composite films after 24 h was slightly lower than that after 12 h. This was because in the high-humidity environment, a large amount of water was absorbed continuously by hydroxypropyl starch due to its hydrophilicity, leading to the swelling of starch molecules, the destruction of the integrity of network structure, and the reduction of water vapor permeability (Perez-Gallardo et al. 2012).

Solvent resistance and absorption of composite films

The solvent resistance of the MCC/HPS films was shown in this paper using various solvents, such as acetone, petroleum ether, ethyl alcohol, oleic acid, and xylene. All film pieces were soaked in solvents at 30 °C, and after a certain time they were photographed by the camera in Fig. 7. It was interesting to survey that the structure of these films had no obvious changes after 48 h of immersion in the solvent solution. With the increase of MCC content, MCC and hydroxypropyl starch formed a compact network structure, hindering the penetration of solvent into the composite films through the capillary force. In addition, partial deformation of microcrystalline cellulose during the film drying process formed dense networks to resist solvents. According to results in the literature that starch can resist most organic solvents, such as esters, hydrocarbons, and so on (Dai et al. 2017). Solvent absorption results of films are listed in Table 2. For example, a few films appeared to dissolve in ethyl alcohol and acetone, separately absorbed above 10% and about 8% after 48 h, but it still maintained their shapes. Hydroxypropyl starch was likely to dissolve in water, and some starch particles swelled a little in the polar solvents. The excellent solvent resistance of MCC/HPS films can enhance their potential applications in the field of food packaging.

Conclusion

In this paper, composite films of microcrystalline cellulose/hydroxypropyl starch with high tensile strength were prepared, with hydroxypropyl starch as the base material, microcrystalline cellulose as the filler, and glycerol and water as plasticizers. The formation of cross-linked structure was verified by SEM and FT-IR analysis results. With increasing amounts of MCC, glass transition temperature, thermal stability, solvent resistance, and tensile strength of composite films improved, while the moisture absorption and water vapor permeability decreased. The results of DSC and TGA showed that high thermal stability appeared when the MCC content reached 6 wt% and the glass transition temperature of composite films increased to 137.66 °C. The tensile strength of 6 wt% MCC/HPS composite films was improved by about 300% compared with that of HPS films, as shown by test results of mechanical properties. It can be concluded that the moisture absorption and water vapor transmission of composite films decreased over time with increasing amounts of MCC, based on the calculation of the hygroscopicity and water vapor permeability. Apparently, the optimal performance indexes of the prepared MCC/HPS can be obtained with the addition of 6 wt% MCC, thus facilitating the application of hydroxypropyl starch, a starch derivative, in the bio-based plastic packaging field.

Table 2 Solvent absorption of films prepared form HPS and MCC

Types of samples	Acetone (%)	Petroleum ether (%)	Ethyl alcohol (%)	Oleic acid (%)	Xylene (%)
HPS	8.72 ± 0.12	1.57 ± 0.03	14.75 ± 0.31	5.11 ± 0.11	1.27 ± 0.06
3 wt% MCC/HPS	8.53 ± 0.15	1.20 ± 0.05	13.65 ± 0.35	4.87 ± 0.09	1.15 ± 0.03
6 wt% MCC/HPS	7.43 ± 0.07	0.81 ± 0.01	11.46 ± 0.29	4.38 ± 0.07	1.02 ± 0.01
9 wt% MCC/HPS	7.86 ± 0.04	0.89 ± 0.02	12.72 ± 0.18	4.71 ± 0.15	1.04 ± 0.04

Acknowledgments This work was financially supported by the National Natural Science Foundation of China (31270633), the State Key Laboratory of Pulp and Paper Engineering of China (201512), the Lianyungang 555 Talents Project Program of China (2015-13), the Hangzhou Qianjiang Distinguished Experts Programme of China, and a project funded by the Priority Academic Program Development of Jiangsu Higher Education Institutions.

References

Alhuthali A, Low IM, Dong C (2012) Characterisation of the water absorption, mechanical and thermal properties of recycled cellulose fibre reinforced vinyl-ester eco-nanocomposites. Compos Part B Eng 43:2772–2781

Andresen M, Johansson LS, Tanem BS, Stenius P (2006) Properties and characterization of hydrophobized microfibrillated cellulose. Cellulose 13:665–677

Bakrudeen HB, Sudarvizhi C, Reddy BSR (2016) Starch nanocrystals based hydrogel: construction, characterizations and transdermal application. Mat Sci Eng C Mater 68:880–889

Bergo PVA, Carvalho RA, Sobral PJA, dos Santos RMC, da Silva FBR, Prison JM, Solorza-Feria J, Habitante AMQB (2008) Physical properties of edible films based on cassava starch as affected by the plasticizer concentration. Packag Technol Sci 21:85–89

Brandelero RPH, Yamashita F, Grossmann MVE (2010) The effect of surfactant Tween 80 on the hydrophilicity, water vapor permeation, and the mechanical properties of cassava starch and poly(butylene adipate-co-terephthalate) (PBAT) blend films. Carbohydr Polym 82:1102–1109

Brandelero RPH, Yamashita F, Zanela J, Brandelero EM, Caetano JG (2015) Mixture design applied to evaluating the effects of polyvinyl alcohol (PVOH) and alginate on the properties of starch-based films. Starch-Starke 67:191–199

Brandelero RPH, Brandelero EM, de Almeida FM (2016) Biodegradable films of starch/PVOH/alginate in packaging systems for minimally processed lettuce (*Lactuca sativa* L.). Cienc Agrotech 40:510–521

Brannan RG, Mah E, Schott M, Yuan SM, Casher KL, Myers A, Herrick C (2014) Influence of ingredients that reduce oil absorption during immersion frying of battered and breaded foods. Eur J Lipid Sci Technol 116:240–254

Cervantes-Sanchez JJ, Rico-Martinez JM, Perez-Munoz VH (2016) Angularity and axiality of a Schonflies parallel manipulator. Robotica 34:2415–2439

Czaja WK, Young DJ, Kawecki M, Brown RM (2007) The future prospects of microbial cellulose in biomedical applications. Biomacromol 8:1–12

Dai L, Long Z, Chen J, An X, Cheng D, Khan A, Ni Y (2017) Robust guar gum/cellulose nanofibrils multilayer films with good barrier properties. ACS Appl Mater Interfaces 9:5477–5485

Dufresne A, Vignon MR (1998) Improvement of starch film performances using cellulose microfibrils. Macromolecules 31:2693–2696

Dufresne A, Dupeyre D, Vignon MR (2000) Cellulose microfibrils from potato tuber cells: processing and characterization of starch-cellulose microfibril composites. J Appl Polym Sci 76:2080–2092

Edhirej A, Sapuan SM, Jawaid M, Zahari NI (2017) Effect of various plasticizers and concentration on the physical, thermal, mechanical, and structural properties of cassava-starch-based films. Starch-Starke 69(1–2)

Fouladi E, Nafchi AM (2014) Effects of acid-hydrolysis and hydroxypropylation on functional properties of sago starch. Int J Biol Macromol 68:251–257

Frone AN, Nicolae CA, Gabor RA, Panaitescu DM (2015) Thermal properties of water-resistant starch–polyvinyl alcohol films modified with cellulose nanofibers. Polym Degrad Stab 121:385–397

Fukuzumi H, Saito T, Isogai A (2013) Influence of TEMPO-oxidized cellulose nanofibril length on film properties. Carbohydr Polym 93:172–177

Guz L, Fama L, Candal R, Goyanes S (2017) Size effect of ZnO nanorods on physicochemical properties of plasticized starch composites. Carbohydr Polym 157:1611–1619

Ismail H, Zaaba NF (2014) Effects of poly(vinyl alcohol) on the performance of sago starch plastic films. J Vinyl Addit Technol 20:72–79

Jang WY, Shin BY, Lee TX, Narayan R (2007) Thermal properties and morphology of biodegradable PLA/starch compatibilized blends. J Ind Eng Chem 13:457–464

Kaushik A, Kaur R (2016) Thermoplastic starch nanocomposites reinforced with cellulose nanocrystals: effect of plasticizer on properties. Compos Interface 23:701–717

Lani NS, Ngadi N, Johari A, Jusoh M (2014) Isolation, characterization, and application of nanocellulose from oil palm empty fruit bunch fiber as nanocomposites. J Nanomater 2014:1687–4110

Lavoine N, Desloges I, Dufresne A, Bras J (2012) Microfibrillated cellulose—its barrier properties and applications in cellulosic materials: a review. Carbohydr Polym 90:735–764

Lawal OS (2011) Hydroxypropylation of pigeon pea (*Cajanus cajan*) starch: preparation, functional characterizations and enzymatic digestibility. LWT Food Sci Technol 44:771–778

Lee HL, Yoo B (2011) Effect of hydroxypropylation on physical and rheological properties of sweet potato starch. LWT Food Sci Technol 44:765–770

Lim KS, Bee ST, Sin LT, Tee TT, Ratnam CT, Hui D, Rahmat AR (2016) A review of application of ammonium polyphosphate as intumescent flame retardant in thermoplastic composites. Compos Part B Eng 84:155–174

Liu DG, Sun X, Tian HF, Maiti S, Ma ZS (2013) Effects of cellulose nanofibrils on the structure and properties on PVA nanocomposites. Cellulose 20:2981–2989

Liu DG, Ma ZS, Wang ZM, Tian HF, Gu MY (2014) Biodegradable poly(vinyl alcohol) foams supported by cellulose nanofibrils: processing, structure, and properties. Langmuir 30:9544–9550

Lu J, Wang T, Drzal LT (2008) Preparation and properties of microfibrillated cellulose polyvinyl alcohol composite materials. Compos Part A: Appl Sci Manuf 39:738–746

Ma XF, Yu JG, Kennedy JF (2005) Studies on the properties of natural fibers-reinforced thermoplastic starch composites. Carbohydr Polym 62:19–24

Mondragon G, Pena-Rodriguez C, Gonzalez A, Eceiza A, Arbelaiz A (2015) Bionanocomposites based on gelatin matrix and nanocellulose. Eur Polym J 62:1–9

Perez-Gallardo A, Bello-Perez LA, Garcia-Almendarez B, Montejano-Gaitan G, Barbosa-Canovas G, Regalado C (2012) Effect of structural characteristics of modified waxy corn starches on rheological properties, film-forming solutions, and on water vapor permeability, solubility, and opacity of films. Starch-Starke 64:27–36

Rahman WAWA, Sin LT, Rahmat AR, Samad AA (2010) Thermal behaviour and interactions of cassava starch filled with glycerol plasticized polyvinyl alcohol blends. Carbohydr Polym 81:805–810

Ramaraj B (2006) Modified poly(vinyl alcohol) and coconut shell powder composite films: physico-mechanical, thermal properties, and swelling studies. Polym Polym Plast Technol 45:1227–1231

Ramesan MT, Surya K (2016) Synthesis, characterization, and properties of cashew gum graft poly(acrylamide)/magnetite nanocomposites. J Appl Polym Sci 133:43496–43503

Rico M, Rodriguez-Llamazares S, Barral L, Bouza R, Montero B (2016) Processing and characterization of polyols plasticized-starch reinforced with microcrystalline cellulose. Carbohydr Polym 149:83–93

Rodionova G, Roudot S, Eriksen O, Mannle F, Gregersen O (2012) The formation and characterization of sustainable layered films incorporating microfibrillated cellulose (MFC). BioResources 7:3690–3700

Siqueira G, Bras J, Dufresne A (2010) Cellulosic bionanocomposites: a review of preparation, properties and applications. Polym Basel 2:728–765

Siro I, Plackett D (2010) Microfibrillated cellulose and new nanocomposite materials: a review. Cellulose 17:459–494

Sobral PJD, dos Santos JS, Garcia FT (2005) Effect of protein and plasticizer concentrations in film forming solutions on physical properties of edible films based on muscle proteins of a Thai Tilapia. J Food Eng 70:93–100

Svagan AJ, Hedenqvist MS, Berglund L (2009) Reduced water vapour sorption in cellulose nanocomposites with starch matrix. Compos Sci Technol 69:500–506

Veigel S, Muller U, Keckes J, Obersriebnig M, Gindl-Altmutter W (2011) Cellulose nanofibrils as filler for adhesives: effect on specific fracture energy of solid wood-adhesive bonds. Cellulose 18:1227–1237

Yakimets I, Paes SS, Wellner N, Smith AC, Wilson RH, Mitchell JR (2007) Effect of water content on the structural reorganization and elastic properties of biopolymer films: a comparative study. Biomacromol 8:1710–1722

Yano H, Nakahara S (2004) Bio-composites produced from plant microfiber bundles with a nanometer unit web-like network. J Mater Sci 39:1635–1638

Yoon SD, Park MH, Byun HS (2012) Mechanical and water barrier properties of starch/PVA composite films by adding nano-sized poly(methyl methacrylate-co-acrylamide) particles. Carbohydr Polym 87:676–686